

Production of gluons in the classical field model for heavy ion collisions

T. Lappi*

*Department of Physical Sciences, Theoretical Physics Division and
 Helsinki Institute of Physics
 P.O. Box 64, FIN-00014 University of Helsinki, Finland*

The initial stages of relativistic heavy ion collisions are studied numerically in the framework of a 2+1 dimensional classical Yang-Mills theory. We calculate the energy and number densities and momentum spectra of the produced gluons. The model is also applied to noncentral collisions. The numerical results are discussed in the light of RHIC measurements of energy and multiplicity and other theoretical calculations. Some problems of the present approach are pointed out.

PACS numbers: 24.85.+p, 25.75.-q, 12.38.Mh

I. INTRODUCTION

In ultrarelativistic heavy ion collisions such as studied at RHIC and LHC particle production in the central rapidity region is dominated by the gluonic degrees of freedom in the nucleus. At sufficiently small x the phase space density of these gluons is large, so one can try to treat them as a classical color field. Let us first briefly review the model of [1, 2, 3] before turning to our results in Sec. IV and their phenomenological implications in Sec. V. Our notation is essentially that of [1, 2, 3].

The idea of [1] was to model the high momentum degrees of freedom of a nucleus as static random classical color sources with a Gaussian probability distribution:

$$\langle \rho^a(x_T) \rho^b(y_T) \rangle = g^2 \mu^2 \delta^{ab} \delta^2(x_T - y_T), \quad (1)$$

where x_T and y_T are vectors in the transverse plane. The classical color field generated by this source is then obtained from the equations of motion

$$[D_\mu, F^{\mu\nu}] = J^\nu. \quad (2)$$

This original formulation of the model is very simple, beyond the nuclear radius R_A it only depends on one dimensional phenomenological parameter μ (related to Λ_s introduced in [4] by $\Lambda_s = g^2 \mu$) and the QCD coupling g that does not run in this classical approximation. One may, however, argue that the Gaussian probability distribution should be replaced by something else, namely a solution of the ‘‘JIMWLK’’ renormalization group equation [5].

The McLerran-Venugopalan model [1] describes the wave function of one nucleus. Nucleus-nucleus collisions were first studied in this framework in [2]. The source current is taken to be

$$J^\mu = \delta^{\mu+} \rho_{(1)}(x_T) \delta(x^-) + \delta^{\mu-} \rho_{(2)}(x_T) \delta(x^+), \quad (3)$$

where the color charge densities $\rho_{(m)}$ of the two nuclei are independent. In the region $x^- < 0$, $x^+ < 0$ which is

causally connected to neither of the nuclei, the solution can be chosen as $A_\mu = 0$. In the regions $x^- < 0$, $x^+ > 0$ and $x^- > 0$, $x^+ < 0$ which are causally connected to only one of the nuclei the solutions are ‘‘transverse pure gauges’’

$$A_{(m)}^i = -\frac{i}{g} e^{i\Lambda_{(m)}} \partial^i e^{-i\Lambda_{(m)}}, \quad \text{with } \nabla_T^2 \Lambda_{(m)} = -g\rho_{(m)}. \quad (4)$$

The initial condition ($\tau = 0$) for the interesting region $x^- > 0$, $x^+ > 0$ is obtained by matching the solutions on the light cone. This yields:

$$\begin{aligned} A^i|_{\tau=0} &= A_{(1)}^i + A_{(2)}^i, \\ A^\eta|_{\tau=0} &= \frac{ig}{2} [A_{(1)}^i, A_{(2)}^i]. \end{aligned} \quad (5)$$

Modeling the sources as delta functions on the light cone (Eq. (3)) makes the initial conditions boost invariant. We shall also restrict ourselves to strictly boost invariant field configurations. This elimination of the longitudinal degrees of freedom makes the numerical solution of the equations of motion easier, but is a serious limitation, especially for studying thermalisation (see e.g. [6]).

II. (2+1)-DIMENSIONAL CLASSICAL HAMILTONIAN CHROMODYNAMICS ON THE LATTICE

The analytic solution of the equations of motion, Eq. (2), with the initial conditions, Eqs. (5), is not known, but they can be studied numerically. A lattice Hamiltonian formulation of the model was first developed in [3].

Assuming that the field configurations are boost-invariant reduces the system to a 2+1-dimensional one. Choosing the Schwinger gauge $A_\tau = 0$ one can cast the equations of motion into a Hamiltonian form. The lattice

*Email address: tuomas.lappi@helsinki.fi

Hamiltonian is:

$$aH = \sum_{x_T} \left\{ \frac{g^2 a}{\tau} \text{Tr} E^i E^i + \frac{2N_c \tau}{g^2 a} \left(1 - \frac{1}{N_c} \text{Re} \text{Tr} U_\perp \right) + \frac{\tau}{a} \text{Tr} \pi^2 + \frac{a}{\tau} \sum_i \text{Tr} \left(\phi - \tilde{\phi}_i \right)^2 \right\}, \quad (6)$$

where a is the lattice spacing and E_i, U_i, π and ϕ are dimensionless lattice fields. The fields are matrices in color space, with $E^i = E_a^i t_a$ etc. and the generators of the fundamental representation normalised in the conventional way as $\text{Tr} t_a t_b = 1/2 \delta_{ab}$. The first two terms are the transverse electric and magnetic fields, with the transverse plaquette

$$U_\perp(x_T) = U_x(x_T) U_y(x_T + e_x) U_x^\dagger(x_T + e_y) U_y^\dagger(x_T). \quad (7)$$

The last two terms are the kinetic energy and covariant derivative of the rapidity component of the gauge field $\phi \equiv A_\eta = -\tau^2 A^\eta$, which becomes an adjoint representation scalar with the assumption of boost invariance. For the parallel transported scalar field we have used the notation

$$\tilde{\phi}_i(x_T) \equiv U_i(x_T) \phi(x_T + e_i) U_i^\dagger(x_T). \quad (8)$$

In the Hamiltonian, Eq. (6), there is a residual invariance under gauge transformations depending only on the

transverse coordinates. The Hamiltonian equations of motion are

$$\dot{U}_i = i \frac{g^2}{\tau} E^i U_i \text{ (no sum over } i), \quad (9)$$

$$\dot{\phi} = \tau \pi, \quad (10)$$

$$\dot{E}^x = \frac{i\tau}{2g^2} [U_{x,y} + U_{x,-y} - \text{h.c.}] - \text{trace} + \frac{i}{\tau} [\tilde{\phi}_x, \phi] \quad (11)$$

$$\dot{E}^y = \frac{i\tau}{2g^2} [U_{y,x} + U_{y,-x} - \text{h.c.}] - \text{trace} + \frac{i}{\tau} [\tilde{\phi}_y, \phi],$$

$$\dot{\pi} = \frac{1}{\tau} \sum_i [\tilde{\phi}_i + \tilde{\phi}_{-i} - 2\phi]. \quad (12)$$

The Gauss law, conserved by the equations of motion, reads:

$$\sum_i \left[U_i^\dagger(x_T - e_i) E^i(x_T - e_i) U_i(x_T - e_i) - E^i(x_T) \right] - i[\phi, \pi] = 0. \quad (13)$$

On the lattice the initial conditions (5) become:

$$0 = \text{Tr} \left[t_a \left((U_i^{(1)} + U_i^{(2)}) (1 + U_i^\dagger) - \text{h.c.} \right) \right], \quad (14)$$

$$E^i = 0, \quad (15)$$

$$\phi = 0, \quad (16)$$

$$\pi(x_T) = \frac{-i}{4g} \sum_i \left[(U_i(x_T) - 1) (U_i^{\dagger(2)}(x_T) - U_i^{\dagger(1)}(x_T)) + (U_i^\dagger(x_T - e_i) - 1) (U_i^{(2)}(x_T - e_i) - U_i^{(1)}(x_T - e_i)) - \text{h.c.} \right], \quad (17)$$

where $U^{(1,2)}$ in Eq. (14) are the link matrices corresponding to the color fields of the two nuclei ($A_i^{(1,2)}$ in Eq. (4)) and the link matrix U_i corresponding to the $\tau \geq 0$ color field A_i must be solved from Eq. (14).

The model has three free parameters, the coupling g , the source density μ and the nuclear transverse area πR_A^2 . In this work the lattice size is taken to be $L^2 = N^2 a^2 = \pi R_A^2$. This means that the field modes have an infrared cutoff of the order $1/R_A$, while physically one would expect them to be cut off at a scale $\sim \Lambda_{\text{QCD}}$ by confinement physics not included in the classical field model. So in order to be physically sensible our results should not depend on this infrared cutoff.

The values of the three parameters g , μ and πR_A^2 separately are needed when translating lattice units to physical units, but the dimensionless parameter $g^2 \mu R_A$ controls the qualitative behavior of the model; the weak coupling or weak field limit is reached for small values of this parameter (see also [7]). To see this consider the system on a transverse lattice of spacing a . Now we have $\delta^2(x_T) \sim 1/a^2$. Thus, from Eq. (1), the charge density $\rho \sim g\mu/a$. The Green's function of the operator ∇_T^2 in Eq. (4) is a logarithm, which is parametrically constant. Thus $\Lambda(x_T)$ is obtained by summing contributions $\sim g \cdot a^2 \cdot g\mu/a$ from each of the $\sim R_A^2/a^2$ cells (the area of a cell being a^2). Because the charges are distributed as

Gaussians with zero expectation value, their sum scales as a square root of the number of lattice sites, and we get $\Lambda(x_T) \sim ag^2\mu \cdot \sqrt{R_A^2/a^2} \sim g^2\mu R_A$. Because of the exponentials of Λ in Eq. (4) it is the magnitude of the dimensionless field Λ that determines the nonlinearity of the model.

The same argument can also be formulated in momentum space. The Poisson equation, Eq. (4), can be written as $k_T^2 \Lambda(k_T) = g\rho(k_T)$. One needs a prescription to deal with the zero mode, the one chosen here is color neutrality of the system as whole, $\rho(k_T = 0_T) = 0 = \Lambda(k_T = 0_T)$. Then the dominant contribution comes from the smallest nonzero Fourier mode, $k_T \sim 1/R_A$. In momentum space the correlator (1) is $\langle \rho(k_T)\rho(p_T) \rangle \sim g^2\mu^2\delta^2(k_T + p_T)$ with $\delta^2(k_T) \sim R_A^2$. Thus $\Lambda(k_T) \sim gR_A^2\rho(k_T) \sim gR_A^2 \cdot g\mu R_A$ and $\Lambda(x_T) \sim \Lambda(k_T)/R_A^2 \sim g^2\mu R_A$.

In this Hamiltonian formalism the energy per unit rapidity in different field components is naturally the easiest and the most fundamental quantity to compute. One can also measure equal time correlation functions of fields:

$$\langle E_i^a(k_T, \tau) E_i^a(-k_T, \tau) \rangle, \quad (18)$$

$$\langle A_i^a(k_T, \tau) A_i^a(-k_T, \tau) \rangle, \quad (19)$$

$$\langle \pi^a(k_T, \tau) \pi^a(-k_T, \tau) \rangle, \quad (20)$$

$$\langle \phi^a(k_T, \tau) \phi^a(-k_T, \tau) \rangle. \quad (21)$$

These correlation functions are not gauge invariant. One can, however, argue that in the Coulomb gauge $\partial_i A_i = 0$ a physical meaning can be assigned to them (see also [8]). Using equal time field correlation functions one can define a gluon number density $n(k_T)$, but the definition is not unique. The question of defining the number density is discussed in the following section.

III. PARTICLES IN A CLASSICAL FIELD

In a weakly interacting scalar theory it is easy to define a particle number corresponding to a given classical field configuration. Take a free Hamiltonian and Fourier transform it:

$$\begin{aligned} H &= \int d^d x \left[\frac{1}{2} \pi^2(x) + \frac{1}{2} (\nabla \phi)^2(x) + \frac{1}{2} m^2 \phi^2 \right] \quad (22) \\ &= \int \frac{d^d k}{(2\pi)^d} \left[\frac{1}{2} |\pi(k)|^2 + \frac{1}{2} \omega^2(k) |\phi(k)|^2 \right] \\ &= \int d^d k \omega(k) n(k), \quad (23) \end{aligned}$$

with the free dispersion relation $\omega^2(k) = k^2 + m^2$. Averaged in time the energy is distributed equally between the degrees of freedom:

$$\overline{\frac{1}{2} |\pi(k)|^2} = \overline{\frac{1}{2} \omega^2(k) |\phi(k)|^2} \quad (24)$$

so we can identify:

$$\overline{|\pi(k)|^2} = \omega(k) n(k), \quad \overline{|\phi(k)|^2} = \frac{n(k)}{\omega(k)}. \quad (25)$$

For an interacting theory one can *define* the number distribution as follows:

$$n(k) = \sqrt{\overline{|\pi(k)|^2} \overline{|\phi(k)|^2}}, \quad \omega(k) = \sqrt{\frac{\overline{|\pi(k)|^2}}{\overline{|\phi(k)|^2}}}. \quad (26)$$

There is also another possibility, we can also *assume* a dispersion relation $\omega_{\text{free}}(k) = \sqrt{m^2 + k^2}$ and define

$$n(k) = \frac{\overline{|\pi(k)|^2}}{\omega_{\text{free}}(k)}. \quad (27)$$

The latter approach is the one we take. Explicitly, for this particular theory described by the Hamiltonian, Eq. (6), a 2-dimensional gauge field with an adjoint representation scalar field on the lattice, we define

$$n(k_T) = \frac{2}{N^2} \frac{1}{\tilde{k}} \left[\frac{g^2}{2\tau} E_i^a(k_T) E_i^a(-k_T) + \frac{\tau}{2} \pi^a(k_T) \pi^a(-k_T) \right], \quad (28)$$

where

$$\tilde{k}^2 = \frac{4}{a^2} \left[\sin^2 \frac{ak_x}{2} + \sin^2 \frac{ak_y}{2} \right] \quad (29)$$

is the free, massless lattice dispersion relation. We can then verify that our method is consistent with the approach of Eq. (26) by looking at the correlation functions

$$\frac{1}{\tau} \sqrt{\frac{\langle E_i^a(k_T) E_i^a(-k_T) \rangle}{\langle A_i^a(k_T) A_i^a(-k_T) \rangle}} \quad \text{and} \quad \tau \sqrt{\frac{\langle \pi^a(k_T) \pi^a(-k_T) \rangle}{\langle \phi^a(k_T) \phi^a(-k_T) \rangle}} \quad (30)$$

and verifying that they behave as $\omega(\tilde{k}) \approx \tilde{k}$ (see Fig. 1).

IV. RESULTS

To state our results in a form easily comparable with [4] let us define the same dimensionless quantities f_N and f_E as follows:

$$f_E = \frac{1}{g^4 \pi R_A^2 \mu^3} \frac{dE_{\text{init}}}{d\eta}, \quad (31)$$

$$f_N = \frac{1}{g^2 \pi R_A^2 \mu^2} \frac{dN_{\text{init}}}{d\eta}. \quad (32)$$

As discussed in Sec. II the quantities f_E and f_N are functions of only one dimensionless variable $g^4 \pi R_A^2 \mu^2$. In the weak field limit, namely for $\sqrt{g^4 \pi R_A^2 \mu^2} \lesssim 50$, f_E and f_N have a strong dependence on $g^4 \pi R_A^2 \mu^2$. This signals a dependence on the infrared cutoff of the theory. In the strong field limit, i.e. at large enough values of $g^4 \pi R_A^2 \mu^2$,

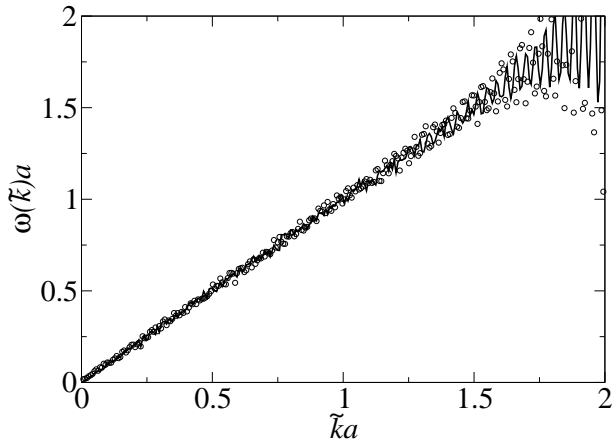


FIG. 1: The functions (30). The circles are $\omega(\tilde{k})$ determined from the transverse fields E^i and A_i , the solid line is $\omega(\tilde{k})$ determined from π and ϕ . The maximum value of $\tilde{k}a$ is $2\sqrt{2}$.

the nonlinearities of the infrared modes regulate this infrared divergence and f_E and f_N become approximately independent of $g^4\pi R_A^2\mu^2$, as can be seen from Fig. 2. Our results for the energy and multiplicity are summarized in Figs. 2 and 3 and Table I. The total energy as a function of time in different field components is plotted in Fig. 4 and the energy in the different field components in Fig. 5.

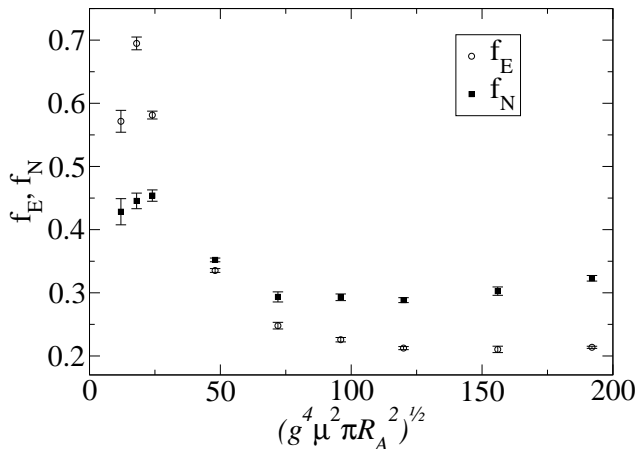


FIG. 2: The functions f_E and f_N as defined by Eqs. (31), (32) vs. $\sqrt{g^4\mu^2\pi R_A^2}$. Computed on a 256^2 -lattice.

Our result for f_E is smaller than that of [4] by approximately a factor of two. The function $dN/d^2k_T(k_T)$ we obtain is different although its integral over k_T -space,

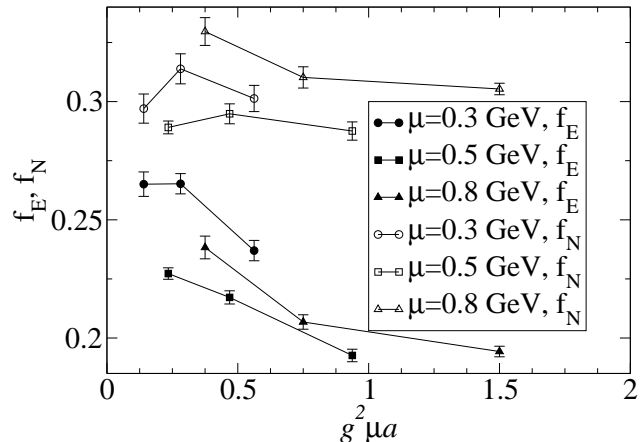


FIG. 3: The functions f_E and f_N defined by Eqs. (31), (32) for constant $\sqrt{g^4\mu^2\pi R_A^2}$ and with different lattice spacings. The horizontal axis is $g^2\mu a$, so the continuum ($a \rightarrow 0$) limit is obtained by extrapolating each set of points to the $g^2\mu a = 0$ -axis on the left.

$\sqrt{g^4\mu^2\pi R_A^2}$	μ (GeV)	f_E	f_N
72	0.29	0.265 ± 0.005	0.297 ± 0.006
120	0.49	0.227 ± 0.003	0.289 ± 0.003
192	0.78	0.238 ± 0.005	0.329 ± 0.006

TABLE I: The values for f_N and f_E corresponding to the points nearest to the continuum limit in Fig. 2. The value of μ in physical units is computed taking $g = 2$ and $\pi R_A^2 = 148 \text{ fm}^2$. The value of f_E is obtained by fitting the energy to a form $A + Be^{-\tau/\tau_0}$ and using the value A . The multiplicity is measured at a time $\tau = 5/\mu$, but its dependence on τ is very weak.

and thus f_N , happens to be the same. This difference is illustrated in Fig. 6.

One can also derive a large k_T analytic expression for the multiplicity in the classical field model [2] [9] (see also [10]). An expansion to the lowest nontrivial order in the field strength gives:

$$\frac{dN}{d\eta d^2k_T} = \frac{\pi R_A^2}{(2\pi)^3} \frac{1}{\pi} \frac{N_c(N_c^2 - 1)g^6\mu^4}{k_T^4} \ln \frac{k_T^2}{\Lambda^2}, \quad (33)$$

with Λ some infrared cutoff. A useful check of the numerical computations is that they should approach the analytic result in the weak field limit of small $g^2\mu R_A$, although the uncertainty from the infrared divergence of the analytical result can be numerically large. Figure 7 shows that we do indeed observe a transition to a perturbative $1/k_T^4 \times$ logarithmic factors – behaviour around $k_T \gtrsim 2g^2\mu$, although in this region the shape of the spectrum is already severely modified by lattice effects, as can be seen comparing the plots for the two

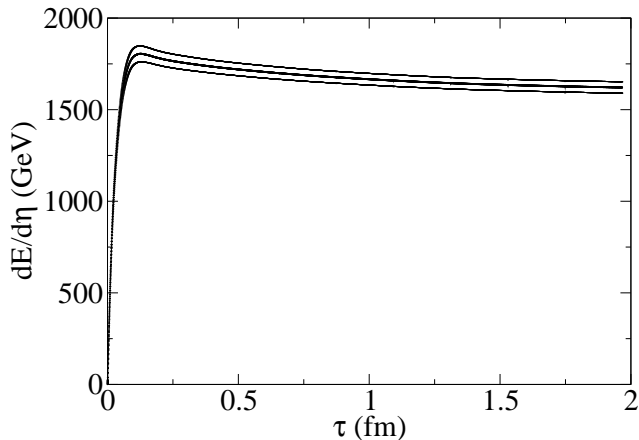


FIG. 4: Total energy per unit rapidity as a function of time for $\mu = 0.5$ GeV. The three curves give an error estimate from 5 trajectories on a 512^2 -lattice.

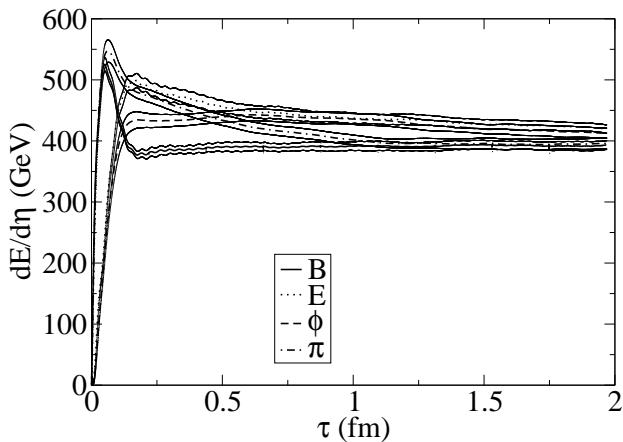


FIG. 5: Energy in different field components from the same simulations as in Fig. 4.

lattice sizes. But, as seen in Fig. 8, the overall normalisation of our numerical result is far away from the analytical result at large $\sqrt{g^4\mu^2\pi R_A^2}$ and approaches it only for $\sqrt{g^4\mu^2\pi R_A^2} \lesssim 10$. This would suggest that the weak field approximation used to obtain the analytical result (33) is unsuitable for a quantitative understanding of this classical field model, whose justification lies, after all, in the argument of strong fields.

Our definition of the gluon number spectrum, Eq. (28), is based on equal time correlators of fields. These correlators are gauge dependent, which is a fundamental difficulty in defining a multiplicity of gluons for this clas-

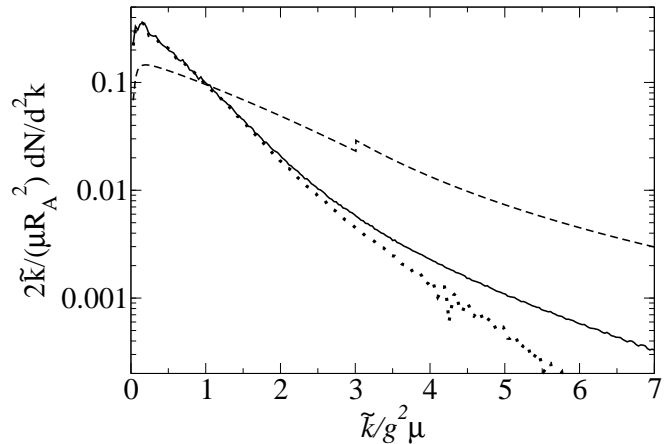


FIG. 6: $\frac{2\tilde{k}}{\mu R_A^2} \frac{dN}{d^2k_T}$ as a function of $\tilde{k}/g^2\mu$ for $\sqrt{g^4\mu^2\pi R_A^2} = 120$. The solid line is our result for a 512^2 -lattice, the dotted line for a 256^2 -lattice and the dashed line a fit to the numerical result of [4]. The area under the curves (which is just f_N defined in Eq. (32)) is approximately the same (although the logarithmic scale makes this hard to see). The dashed curve practically falls on top of the solid one if the vertical axis is scaled by 2 and the horizontal by $1/2$ — a signal of a difference in the normalisation.

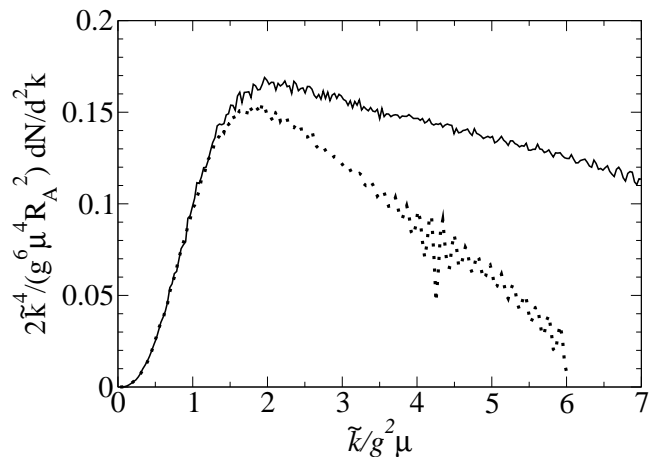


FIG. 7: $\frac{2\tilde{k}^4}{g^6\mu^4 R_A^2} \frac{dN}{d^2k_T}$ as a function of $\tilde{k}/g^2\mu$ from the same simulations as Fig. 6. The solid line is our result for a 512^2 -lattice and the dotted line for a 256^2 -lattice.

sical field model. We have studied this gauge dependence by using as an example the electric field correlator $\langle E_i^a(k_T)E_i^a(-k_T) \rangle$, which is plotted in Fig. 9. Its gauge dependence is limited mainly by the constraint that the

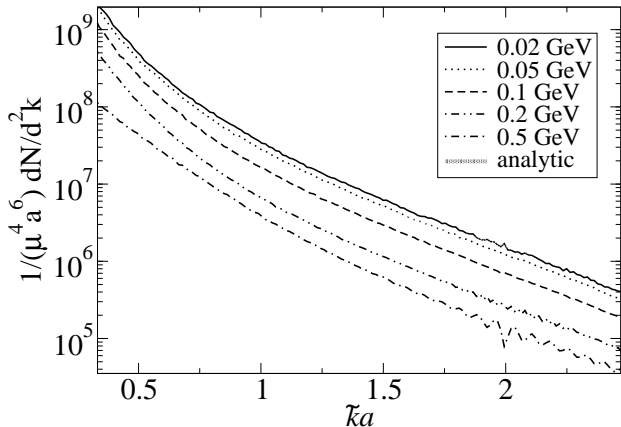


FIG. 8: $\frac{1}{\mu^4 a^6} \frac{dN}{d^2k}$ as a function of $\tilde{k}a$ plotted for $\sqrt{g^4 \mu^2 \pi R_A^2} = 240 \mu / \text{GeV}$ with values of μ given in the figure, compared with the analytical continuum result, Eq. (33).

integral

$$\int d^2k_T E_i^a(k_T) E_i^a(-k_T), \quad (34)$$

which is proportional to the energy in the electric field, is gauge independent.

To determine the multiplicity using Eq. (28) we take the fields resulting from the initial conditions, Eqs. (14) and evolve them in time according to the equations of motion, Eqs. (9). The “no gauge fixing”-curve in Fig. 9 shows the $\langle E_i^a(k_T) E_i^a(-k_T) \rangle$ -correlator obtained in this way. The fields are then gauge transformed into the two dimensional Coulomb gauge $\partial_i A_i = 0$ to get the “Coulomb gauge”-correlator, also plotted in Fig. 9. This is the one that is used to determine the multiplicity. In Fig. 9 we also plot the same correlator in two other gauges, $\partial_x A_x = 0$ and a “Coulomb + random” gauge, which is obtained by taking a field configuration in the Coulomb gauge and performing an independent random gauge transformation on each lattice site. In the latter the independent (Gaussian in this case) transformations on each lattice site naturally enhance the high momentum parts of the spectrum.

According to the discussion in Sec V the value of the parameter μ relevant to RHIC phenomenology would be $\mu = 0.5 \text{ GeV}$ or $\Lambda_s = 2 \text{ GeV}$. One can then ask whether this is indeed in the domain of validity of the present model, i.e. whether the occupation numbers of gluons are high enough. To address this question we plot in Fig. 10 the two dimensional phase space density $f(k_T) = \frac{1}{2(N_c^2 - 1)} \frac{(2\pi)^2}{\pi R_A^2} \frac{dN}{d^2k_T}$, where the spin and color degeneracy has been divided out. It is of order one only up to momenta of a fraction of $g^2 \mu$, meaning that the as-

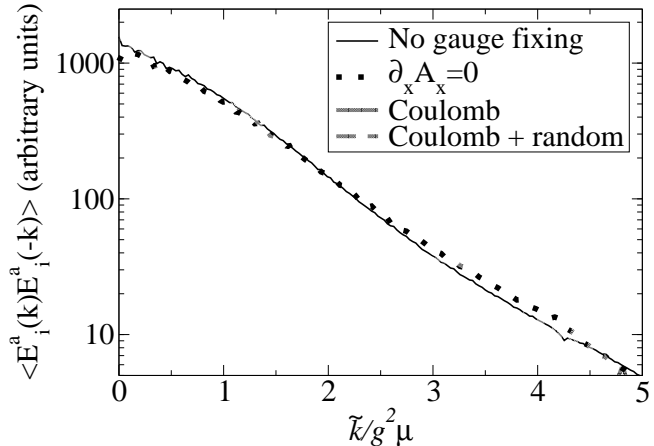


FIG. 9: The correlator $\langle E_i^a(k_T) E_i^a(-k_T) \rangle$ in different gauges: the correlator resulting from the initial conditions and the equations of motion without additional gauge fixing, in “partial Coulomb” $\partial_x A_x = 0$ gauge, in the Coulomb gauge $\partial_i A_i = 0$ and in a gauge obtained by a random gauge transformation of the Coulomb gauge field.

sumption of high occupation numbers is only marginally satisfied.

Seeing that the results of [4, 11] are in many aspects qualitatively similar to ours and after a comparison of the numerical methods it seems that the difference in our results concerning the energy and the number spectrum are simply due to a different normalisation of the $SU(3)$ generators (compare Eq. (6) and Eq. (A5) of [11]). Any phenomenological discussion, such as the following, cannot be considered as an argument for the correctness of one or the other numerical result.

V. PHENOMENOLOGY

A. What to expect

To discuss the phenomenological implications of these results in the light of RHIC experiments [12] one must relate the calculated initial multiplicities and transverse energies to the observed quantities. There are several scenarios that can be used to do this. Let us compare different results with the assumption of early thermalisation and adiabatic expansion that has been successful in explaining particle yields and elliptic flow. In this scenario the initial and final multiplicities, related by entropy conservation, are approximately equal, and we take the total (charged and neutral) multiplicity per unit rapidity to be

$$\frac{dN_{\text{init}}}{d\eta} \approx \frac{dN_{\text{final}}}{d\eta} \approx 1000. \quad (35)$$

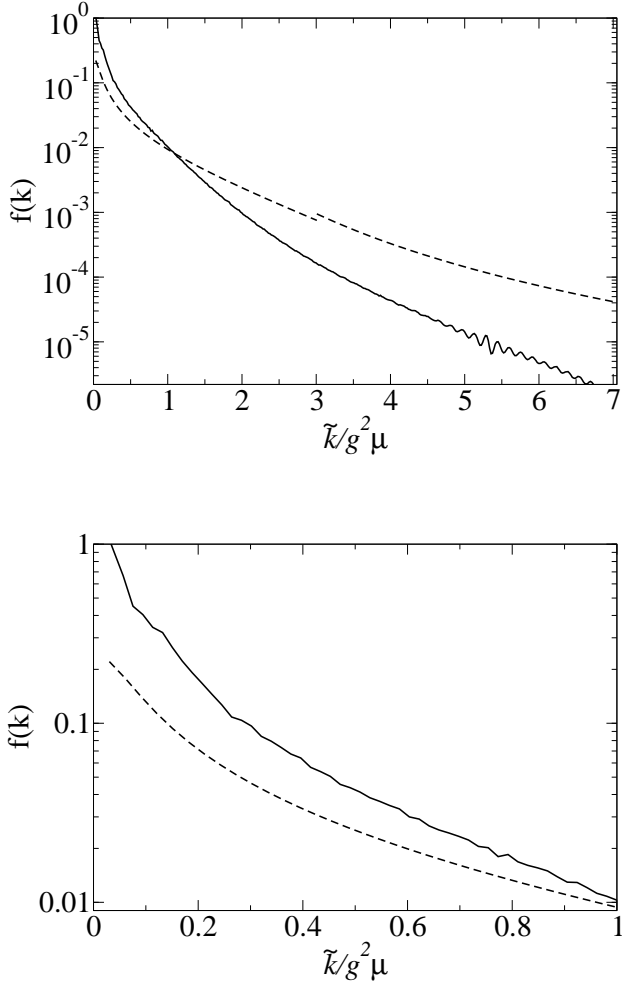


FIG. 10: The two dimensional phase space density $f(k) = \frac{1}{2(N_c^2-1)} \frac{(2\pi)^2}{\pi R_A^2} \frac{dN}{d^2k}$ as a function of $\tilde{k}/g^2\mu$ for $\mu = 0.5$ GeV and $g = 2$, i.e. $\sqrt{g^4\mu^2\pi R_A^2} = 120$. The solid line is our result, the dashed line a fit to the numerical result of [4].

The observed transverse energy is

$$\frac{dE_{\text{final}}}{d\eta} \approx 600 \text{ GeV}. \quad (36)$$

The initial energy is larger than this, due to the expansion of the system. In a freely streaming system the energy per unit rapidity is constant, whereas adiabatic longitudinal expansion makes it decrease as $\tau^{-1/3}$. In [13] the energy is found to be reduced by a factor of 3.5. Because the calculation of [13] is done assuming a very early thermalization it gives an upper bound to the reduction. This translates into a bound for the initial transverse energy $\frac{dE_{\text{init}}}{d\eta} \lesssim 2100$ GeV. Thus a conservative estimate assuming “parton-hadron duality”, be it from entropy

conservation or some other mechanism would be

$$\frac{dE_{\text{init}}}{d\eta} \lesssim 2.1 \text{ GeV} \frac{dN}{d\eta}. \quad (37)$$

The final state saturation model of [13] is a pQCD-calculation supplemented by a sharp infrared cutoff determined from a simple geometrical final state saturation argument. The result of the calculation is (Eq. (5) of [13]):

$$p_{\text{sat}} \frac{dN_{\text{init}}}{d\eta} = 0.288 \text{ GeV} A^{1.050} (\sqrt{s})^{0.574}, \quad (38)$$

Setting $dN_{\text{init}}/d\eta$ to 1000 and taking $A = 200$, $\sqrt{s} = 130$ GeV gives $p_{\text{sat}} = 1.23$ GeV. Then, from Eq. (7) of [13], we get

$$\begin{aligned} \frac{dE_{\text{init}}}{d\eta} &= 1.43 p_{\text{sat}} \frac{dN}{d\eta} \\ &= 1.76 \text{ GeV} \frac{dN}{d\eta}. \end{aligned} \quad (39)$$

Intrinsically such an unphysically sharp infrared cutoff should produce too large an average energy per particle, because there are no gluons with $p_T < p_{\text{sat}}$ in the model. The constant coefficient in front of (38) is determined by the parton distributions and is not fitted to match the RHIC data. The result (39) could thus be regarded as a theoretical upper bound on the initial energy.

B. Classical Yang-Mills result

Let us take from Table I the result for $\mu \approx 0.5$ GeV, which is the value of μ that gives approximately the right multiplicity. We get

$$\frac{dN_{\text{init}}}{d\eta} = 0.29 g^2 \pi R_A^2 \mu^2. \quad (40)$$

This gives $\mu = 0.48$ GeV or $\Lambda_s = 1.9$ GeV. Then the energy is

$$\frac{dE_{\text{init}}}{d\eta} = 0.23 g^4 \pi R_A^2 \mu^3 \quad (41)$$

$$= 0.79 g^2 \mu \frac{dN_{\text{init}}}{d\eta} \quad (42)$$

$$= 1.5 \text{ GeV} \frac{dN_{\text{init}}}{d\eta}. \quad (43)$$

This is well within the bound (37).

The result of [4] is $f_N = 0.3$. Setting $dN_{\text{init}}/d\eta = 1000$ this gives us $\Lambda_s R_A = 65$. Taking $\pi R_A^2 = 148 \text{ fm}^2$ this means $\Lambda_s = 1.87$ GeV. For f_E the result in [4] is $f_E = 0.537$ for $\Lambda_s R_A = 25$ and $f_E = 0.497$ for $\Lambda_s R_A = 83.7$. Taking the value $f_E = 0.5$ one gets

$$\frac{dE_{\text{init}}}{d\eta} = 1.67 \Lambda_s \frac{dN_{\text{init}}}{d\eta} \quad (44)$$

$$= 3.1 \text{ GeV} \frac{dN_{\text{init}}}{d\eta}. \quad (45)$$

Thus the average energy per particle is 3.1 GeV, which is very hard to reconcile with the estimate (37) and forces one to either give up the assumptions behind that estimate or conclude that RHIC energies are not in the domain of validity of the classical field model. One can indeed argue, as in [4], that gluon number increasing processes lower the average energy per particle in the subsequent evolution of the system.

VI. FINITE NUCLEI

It is easy to naively generalise the model to finite nuclei. The Gaussian distribution of the random color charges is argued to arise from a sum of independent fluctuating charges. Thus it is the variance $\langle \rho^a(x_T)\rho^b(y_T) \rangle$ that should be proportional to the thickness of the nucleus:

$$\langle \rho^a(x_T)\rho^b(y_T) \rangle = g^2\mu^2\delta_{x_T,y_T}\delta^{ab}T(x_T - x_{T0}) \quad (46)$$

with $T(x_T) \sim \sqrt{R_A^2 - x_T^2}$ (or some more sophisticated thickness function). Note that the normalisation of μ is different from the square nucleus case, here we fix it by the condition

$$\sum_{x_T,y_T} \langle \rho^a(x_T)\rho^b(y_T) \rangle = \delta^{ab}g^2\mu^2\pi R_A^2. \quad (47)$$

One can then proceed as previously. But the problem one encounters is that the colour fields generated by the sources have long Coulomb tails outside the nuclei. In two dimensions the initial colour fields (4) decay only logarithmically away from the nuclei. Physically the colour fields should decay at distances $\sim 1/\Lambda_{\text{QCD}}$ due to confinement physics not contained in this model.

The approach of [14] and [11], also advocated by [15], is to directly address this question by imposing colour neutrality of the sources at a length scale of the order of a nucleon radius. But it is also possible that a proper inclusion of saturation effects in the probability distribution of the initial colour sources might cure this problem. Saturation does, after all, suppress the very long wavelength modes responsible for the long tails.

Exploring the full implications of the ‘‘JIMWLK’’ renormalization group equation for heavy ion collisions is out of the scope of this work, but in the spirit of, e.g., [16] we have tried substituting the correlation function (46) with the following procedure. We take random variables $f^a(x_T)$ distributed as:

$$\langle f^a(x_T)f^b(y_T) \rangle = \delta_{x_T,y_T}\delta^{ab}T(x_T). \quad (48)$$

The original McLerran-Venugopalan model, equation (1) would be obtained with the choice $\rho^a(x_T) = g\mu f^a(x_T)$. Now we Fourier transform and take

$$\rho^a(k_T) = g\mu\sqrt{\frac{\tilde{k}^2}{\tilde{k}^2 + g^4\mu^2}}f^a(k_T). \quad (49)$$

For $\tilde{k} \gg g^2\mu$ this approaches the original McLerran-Venugopalan model, but for $\tilde{k} \ll g^2\mu$ the fluctuations are cut off as $\langle \rho^a(k_T)\rho^b(k_T) \rangle \sim \tilde{k}^2$. Our results for the multiplicity and energy as a function of centrality are plotted in Fig. 11. All data points have been produced with the same number, 10, of configurations, the larger errors seen using the original Gaussian weight function are a signal of its strong dependence on few infrared modes. The discrepancy in the ratio E/N between our results and those of [4, 11] remains also in the finite nucleus case.

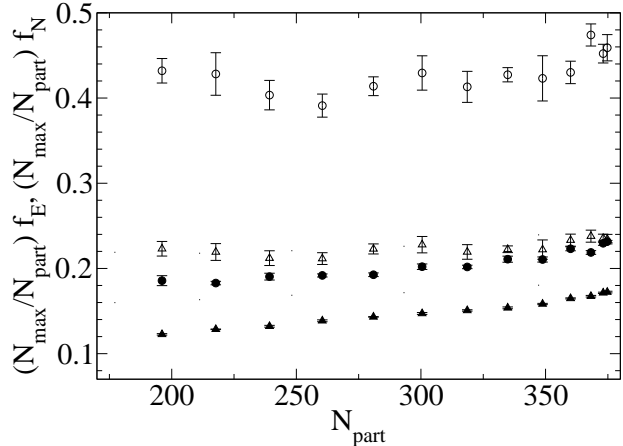


FIG. 11: The functions $\frac{N_{\text{max}}}{N_{\text{part}}} f_N$ (circles) and $\frac{N_{\text{max}}}{N_{\text{part}}} f_E$ (triangles) vs. N_{part} . $N_{\text{max}} \approx 375$ is N_{part} corresponding to impact parameter $b = 0$. The open symbols are results calculated with the original Gaussian weight function and the filled symbols with the saturation ansatz (49). The conversion from b to N_{part} from [17].

In [11] it is said that ‘‘our [using ‘color neutral’ initial conditions] results may be *quantitatively* similar to RG evolved predictions’’. This can also be seen in Fig. 1 of [11], where the neutrality condition originally imposed at the scale Λ_{QCD} has an effect up to the scale $g^2\mu$, leading to a modification of the Gaussian weight function that is very similar to ours. It might thus turn out that at RHIC energies it is not yet possible to distinguish effects from two physically very different phenomena, confinement and saturation.

VII. CONCLUSIONS AND OUTLOOK

We have applied the classical field approach to heavy ion collisions and calculated the energy and number densities and the spectra of the gluons produced in the initial stages of the collisions. We have also extended the model to finite nuclei and experimented with a crude saturation-inspired modification of the original model. The gauge dependence of equal time correlators of the fields which

makes it difficult to define a gluon number density has also been investigated. A more practical difficulty in the model is that the phase space density of particles at RHIC might not yet be large enough to justify its use, i.e. the saturation scale might not be large enough compared to Λ_{QCD} . For hard modes whose phase space density is small one does not even expect a classical field approach to work, and the transition to a pQCD regime should be understood better.

Further things that need to be investigated within this approach include the incorporation of the “JIMWLK” renormalisation group equation into the calculation. A better understanding of thermalisation, if possible within the classical approach, might require extending the study to a 3+1-dimensional model. The “best estimate” in

terms of physical postdictions for RHIC or predictions for LHC phenomenology is not settled yet, but is hopefully converging.

Acknowledgments

The author wishes to thank K. Kajantie for suggesting this topic and his advice, F. Gelis, K. Rummukainen and K. Tuominen for numerous discussions and sharing their expertise and A. Krasnitz, Y. Nara and R. Venugopalan for discussions and correspondence. This work was supported by the Finnish Cultural Foundation and the Academy of Finland (project 77744).

-
- [1] L. McLerran and R. Venugopalan, *Phys. Rev.* **D49** (1994) 2233, hep-ph/9309289; *Phys. Rev.* **D49** (1994) 3352, hep-ph/9311205; *Phys. Rev.* **D50** (1994) 2225, hep-ph/9402335.
 - [2] A. Kovner, L. McLerran and H. Weigert, *Phys. Rev.* **D52** (1995) 3809, hep-ph/9505320; *Phys. Rev.* **D52** (1995) 6231, hep-ph/9502289.
 - [3] A. Krasnitz and R. Venugopalan, *Nucl. Phys.* **B557** (1999) 237, hep-ph/9809433.
 - [4] A. Krasnitz, Y. Nara and R. Venugopalan *Phys. Rev. Lett.* **87** (2001) 192302, hep-ph/0108092.
 - [5] J. Jalilian–Marian, A. Kovner, A. Leonidov and H. Weigert, *Nucl. Phys.* **B504** (1997) 415, hep-ph/9701284; *Phys. Rev.* **D59** (1999) 014014, hep-ph/9706377; J. Jalilian–Marian, A. Kovner, L. McLerran and H. Weigert, *Phys. Rev.* **D55** (1997) 5414, hep-ph/9606337; J. Jalilian–Marian, A. Kovner and H. Weigert, *Phys. Rev.* **D59** (1999) 014015, hep-ph/9709432; E. Iancu, A. Leonidov and L. D. McLerran, *Phys. Lett.* **B510** (2001) 133 hep-ph/0102009; E. Iancu and L. McLerran, *Phys. Lett.* **B510** (2001) 145 hep-ph/0103032; H. Weigert, *Nucl. Phys.* **A703** (2002) 823, hep-ph/0004044; A.H. Mueller, *Phys. Lett.* **B523** (2001) 243, hep-ph/0110169.
 - [6] U. W. Heinz, S. M. Wong, *Phys. Rev.* **C66** (2002) 014907, hep-ph/0205058; nucl-th/0209027.
 - [7] R. V. Gavai and R. Venugopalan, *Phys. Rev.* **D54** (1996) 5795, hep-ph/9605327
 - [8] A. Krasnitz and R. Venugopalan, *Phys. Rev. Lett.* **84** (2000) 4309, hep-ph/9909203; *Phys. Rev. Lett.* **86** (2001) 1717, hep-ph/0007108.
 - [9] M. Gyulassy and L. McLerran, *Phys. Rev.* **C56** (1997) 2219, nucl-th/9704034
 - [10] A. Dumitru and L. McLerran, *Nucl. Phys.* **A 700** (2002) 492, hep-ph/0105268.
 - [11] A. Krasnitz, Y. Nara and R. Venugopalan, *Nucl. Phys.* **A717** (2003) 268, hep-ph/0209269.
 - [12] K. Adcox *et al.* [PHENIX collaboration], *Phys. Rev. Lett.* **87** (2001) 052301, nucl-ex/0104015; C. Adler *et al.* [STAR collaboration], *Phys. Rev. Lett.* **87** (2001) 112303, nucl-ex/0106004; B. B. Back *et al.* [PHOBOS collaboration], *Phys. Rev. Lett.* **87** (2001) 102303, nucl-ex/0106006; I. G. Bearden *et al.* [BRAHMS collaboration], *Phys. Lett.* **B523** (2001) 227, nucl-ex/0108016.
 - [13] K. J. Eskola, K. Kajantie, P. V. Ruuskanen, K. Tuominen, *Nucl. Phys.* **B570** (2000) 379, hep-ph/9909456.
 - [14] A. Krasnitz, Y. Nara and R. Venugopalan, *Phys. Lett.* **B554** (2003) 21, hep-ph/0204361.
 - [15] C. S. Lam and G. Mahlon, *Phys. Rev.* **D64** (2001) 016004, hep-ph/0102337; C. S. Lam, G. Mahlon and W. Zhu, *Phys. Rev.* **D66** (2002) 074005, hep-ph/0207058.
 - [16] E. Iancu, K. Itakura and L. McLerran, hep-ph/0212123.
 - [17] K. Tuominen, private communication.